

# Towards Improving Mission Execution for Autonomous Gliders with an Ocean Model and Kalman Filter

Ryan N. Smith, Jonathan Kelly and Gaurav S. Sukhatme

**Abstract**—Effective execution of a planned path by an underwater vehicle is important for proper analysis of the gathered science data, as well as to ensure the safety of the vehicle during the mission. Here, we propose the use of an unscented Kalman filter to aid in determining how the planned mission is executed. Given a set of waypoints that define a planned path and a discretization of the ocean currents from a regional ocean model, we present an approach to determine the time interval at which the glider should surface to maintain a prescribed tracking error, while also limiting its time on the ocean surface. We assume practical mission parameters provided from previous field trials for the problem set up, and provide the simulated results of the Kalman filter mission planning approach. The results are initially compared to data from prior field experiments in which an autonomous glider executed the same path without pre-planning. Then, the results are validated through field trials with multiple autonomous gliders implementing different surfacing intervals simultaneously while following the same path.

## I. INTRODUCTION

To obtain a synoptic view of dynamic ocean processes, ocean scientists have begun to use autonomous robots to collect data. Surface vehicles have access to GPS, and vehicles that operate close to the sea floor, e.g., SeaBED AUV [1], can use bottom-locking Doppler Velocity Loggers (DVLs) coupled with SLAM to accurately localize the vehicle and collected data for later analysis [2]. There is also a class of vehicles that operate in the middle water column, away from both the surface and sea floor. Here, GPS is unavailable, and either the ocean bottom is too far away for DVL lock, or the on-board sensor suite lacks sufficient high-powered navigation instrumentation.

Autonomous gliders are a prime example platform that falls into this mid-water class. Gliders can spend in excess of 8 hours dead-reckoning under water, navigating by only a compass, magnetometer and depth sensor. Localizing data and reconstructing accurate subsurface glider trajectories can be difficult for long underwater transects. Conversely, frequent surfacing can limit the amount of data that are collected during a deployment by decreasing the total time underwater, and by expending excess energy for communication and localization while on the surface.

The purpose of this paper is to investigate the integration of a Kalman filter with ocean current models to estimate the

dead-reckoning error along a given path. This information is then utilized to determine the most practical surfacing interval to satisfy given mission constraints. This work presents an innovative application of a Kalman filter and ocean model aimed at optimizing the surfacing interval time for autonomous gliders, and other underwater vehicles. Our goal is to ensure that path deviation is constrained below a given threshold, while limiting the number of surfacings.

This approach assumes that the mission waypoints have been preplanned (see Fig. 1), and that general guidelines exist for its execution. We incorporate a kinematic vehicle



Fig. 1. General search area (white polygon) and predetermined path (magenta line) to be executed by an autonomous glider. The yellow lines denote the primary shipping lanes for Long Beach Port; areas that must be avoided. Image created by use of Google Earth

model, simulated sensor measurements and the output from a regional ocean model into an unscented Kalman filter to provide an estimate of the expected error during execution of the given mission. We seek to determine a surfacing interval for the glider, such that a given tracking error is not exceeded. We also require that the glider surfaces within a prescribed distance of each waypoint.

## II. MISSION PLANNING

Mission and path planning for Autonomous Underwater Vehicles (AUVs) is required for a wide variety of applications from ocean observation to marine archaeology. For each type of deployment, an initial mission is generally planned *a priori* to guide the vehicle in an intelligent or optimal manner. Multiple methods exist to generate such paths, e.g., [3], [4], [5], [6], and based on a specific deployment, one or a combination of the cited methods may be used. Given any path, difficulty arises in effectively executing the prescribed

R.N. Smith is with the School of Engineering Systems at the Queensland University of Technology, Brisbane, QLD, 4000 Australia. ryan.smith@qut.edu.au

J. Kelly and G.S. Sukhatme are with the Robotic Embedded Systems Laboratory, Department of Computer Science, University of Southern California, Los Angeles, CA 90089, USA. jonathask@usc.edu, gaurav@usc.edu

motion in an environment as uncertain and complex as the ocean. Generally, focus is on reducing the risk and uncertainty that the vehicle may experience.

We assume a path that is regularly executed by the USC CINAPS [7]. This path, presented in Fig. 1, was designed by ocean scientists with expert domain knowledge for the purpose of assessing long-term variability of physical and biological forcing factors related to phytoplankton blooms in southern California. The six waypoints form a cyclic path of length 97.3 km. For this science-driven application, the synoptic time-scale is  $\sim 120$  hours, i.e., completion time for one cycle. At each surfacing, the glider localizes with GPS and transmits a set data packet for monitoring the vehicle and mission status. Based on prior deployment experience, this process takes  $\sim 15$  min.

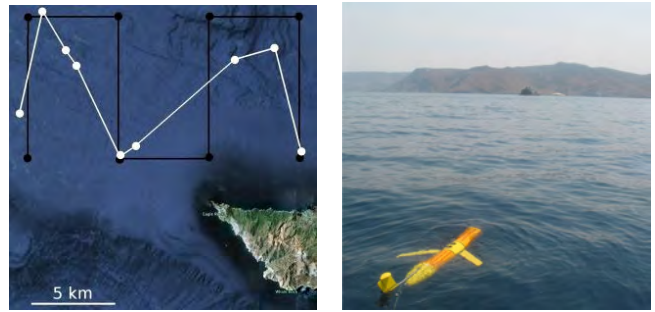
Proper execution of a computed path is crucial to the success of the overall mission. One must consider appropriate regional and vehicular constraints to ensure that the prescribed path can be executed by the vehicle, and is executable with respect to the goals of the mission. For autonomous glider operation in the ocean, we must consider strong and difficult-to-predict currents, infrequent GPS localization, minimal navigational sensors, and non-adaptive behavior while underwater.

A combination of these factors can lead to poor experimental results. For example, Fig. 2(a) displays a planned path in black, and an actual execution of this planned path by a glider in white. The region shown experiences heavy ship traffic, thus surfacings occur at  $> 8$  hour intervals for safety reasons. Additionally, eddies routinely spin up in this region, causing a very complex current regime that render the glider's on-board current correction algorithm minimally helpful. Basing corrections on depth-averaged currents from the previously executed segment, this on-board algorithm cannot accurately predict a circular current. The experimental result presented in Fig. 2(a) is close to a worst-case scenario, but illustrates what can occur without proper consideration for the region of the deployment.

Of primary concern to gliders is the effect of ocean currents. In the region of interest considered in this study, ocean current magnitudes regularly match, and even exceed the operational velocity of the Slocum gliders deployed. Determining an appropriate length of time that a glider should stay submerged between subsequent surfacings for satisfactory execution of a given path is the focus of the remainder of this paper. Next, we present a description of a Slocum glider, the navigational sensor package, and the basic operation of the vehicle.

### A. Autonomous Underwater Gliders

The vehicle for this study is a Webb Slocum autonomous underwater glider [8] as seen in Fig. 2(b). A Slocum glider is a 1.5 m (length) by 21.3 cm (diameter), torpedo-shaped vehicle designed for long-term ( $\sim 1$  month) ocean sampling and monitoring [9], [10]. These vehicles *fly* through the water driven entirely by a variable buoyancy system. Wings convert the buoyancy-dependent vertical motion into forward



(a) Planned lawnmower pattern (black waypoints and path) and the actual executed path (white surfacing locations and path) for a glider deployment off of the northern tip of Santa Catalina Island, CA.

(b) A CINAPS [7] Slocum glider preparing to start a mission off the Northeast coast of Santa Catalina Island, CA.

Fig. 2. 2(a) A sample of a poorly executed path. 2(b) The test-bed vehicle used in this study.

velocity. Inflection points occur at depths and altitudes set in the user-defined mission plan. Thus, the glider navigates by dead-reckoning between waypoints with a sequence of dives and climbs, forming a vertical sawtooth pattern.

Glider are utilized for their deployment endurance, as they provide an optimal method for generating high-resolution spatial and temporal data with minimal energy expense. Sophisticated and power-hungry navigational instruments are not common due to the reduction in deployment duration resulting from their increased power consumption. For similar reasons, on-board decision making and computation are generally not performed. A Slocum glider includes a GPS receiver for localization at each surfacing. For subsurface, dead-reckoning navigation, the vehicle relies on a PNI TCM2 attitude sensor and a SBE 41/41CP pressure sensor. The TCM2 incorporates an electronic compass, a three-axis magnetometer and a two-axis tilt sensor, and is able to provide attitude data at a user-selectable rate of 1 to 30 Hz; heading accuracy is  $\pm 1$  degrees RMS, and roll/pitch accuracy is approximately  $\pm 0.2$  degrees RMS. The SBE sensor measures pressure with an RMS accuracy of 2 decibars, or depth with an RMS accuracy of 2.03 meters near the water surface, at a rate of 1 Hz.

Given their persistence, the data gathered by gliders are important for understanding physical forcing components acting on a regional scale and determining long-term variability [7], [11]. For such applications, we seek techniques to accurately reconstruct and localize the data that are gathered for proper assessment by ocean scientists. Along these lines, methods to increase navigational accuracy of autonomous gliders by use of ocean model predictions have been studied by the authors [12], [13]. These works motivated further research in high-level planning methods to increase the repeatability and reconstructability of executed glider paths.

During a deployment, a Slocum glider navigates by the following method. When navigating to a new waypoint, the present location  $L$  of the vehicle is compared to the next prescribed waypoint in the mission file ( $W_i$ ), and a bearing

and range are computed for execution of the next segment of the mission. The geographical location at the extent of the computed bearing and range from  $L$  is the aiming point  $A_i$ . The vehicle dead-reckons with the computed bearing and range towards  $A_i$ , with the intent of surfacing at  $W_i$ . The computed bearing is not altered, and the glider must surface to make any corrections or modifications to its dive plan. When the glider determines that it has traveled the requested range at the specified bearing (based on speed over ground estimation from the previous dive), it surfaces and acquires a GPS fix. If the vehicle surfaces within a given range of  $W_i$ , the waypoint is determined to be *achieved*. Positional error between the actual surfacing location and  $W_i$  is computed, and is fully attributed to environmental disturbances, i.e., ocean currents. A depth-averaged current vector is computed, and this is factored in when computing the range and bearing to  $W_{i+1}$ . Hence,  $A_i$  is in general not in the same physical location as  $W_i$ , and rarely does the glider ever surface at  $W_i$ .

### B. Problem Description and Setup

There are many user-defined parameters to set for a glider mission: mission waypoints, the pitch angle for diving and ascending ( $\phi$ ), surfacing distance from a given waypoint to consider it *reached* ( $\delta$ ), the maximum duration of time underwater ( $T$ ), minimum and maximum depth range ( $min, max$ ), altitude from the bottom if maximum depth is greater than the water depth, and data transmission preferences. The dive plan parameters are specified in a mission file, and the waypoints are contained in a separate GOTO file. Each mission file calls a specific waypoint list, thus a different set of dive parameters requires the glider to execute a new mission for the same waypoint list. Currently, adaptively changing and executing a new mission plan cannot be done on-board the glider. Missions are uploaded and initiated by a human operator while communicating with the glider while it is on the surface. In the following discussion, we focus our efforts on the choosing the parameter  $T$  for a given mission. The reference mission used is a standard mission executed by the USC CINAPS gliders in the chosen region of interest shown in Fig. 1. The mission considered prescribes ( $min, max$ ) = (5, 80) meters. The waypoints defining the path are shown in Fig. 1.

Given that the area of execution is a coastal region near a densely populated metropolis, there is considerable boat traffic in the area. Previous deployments have been overly cautious in limiting the frequency and duration of surfacings by setting  $T = 8$  hours and sending minimal data packets at each surfacing. The glider then surfaces at each waypoint of the path, or every 8 hours. Operation in this mode can lead to a situation where the 8 hour surfacing requirement occurs just outside of  $\delta$ ; generally set to 1 km. This results in 2 surfacings that are relatively close together, and within a short time period of one another. We would like to avoid this situation to limit unnecessary surfacings, and extended time on the surface. A typical execution of the prescribed path is presented Fig 3.

Over the past three years, the path shown in Fig. 1 has

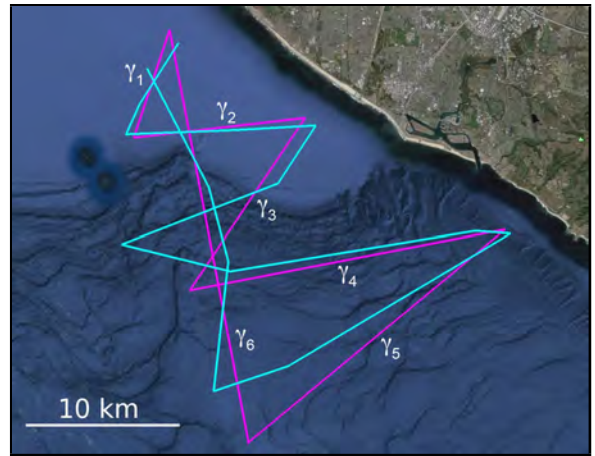


Fig. 3. Typical execution (cyan path) from the data in Table I of the standard reference path (magenta path).

TABLE I  
HISTORICAL EXECUTION STATISTICS FOR THE REFERENCE PATH

Standard Reference Path	Mean and Standard Deviation	Min.	Max.
Prescribed Path Length (km)	97.3	-	-
Actual Distance Traveled (km)	$93.51 \pm 4.58$	86.3	102
Total Traversal Time (hhh:mm)	$110 : 02 \pm 019 : 58$	87	153
Navigation Score (km <sup>2</sup> )	$70.35 \pm 13.35$	56.02	99.7
Navigation Score per km traveled (km)	$0.76 \pm 0.16$	0.59	1.08

been implemented more than 50 times during multiple deployments testing different operational modes and execution methods. Table I presents an analysis of 10 recent path executions that were executed with the assumed standard mission format described earlier.

The navigation score listed in Table I is computed by delineating the glider's executed path (connecting sequential surfacing locations), then computing the absolute area between the executed and prescribed paths. A smaller score indicates less deviation from the prescribed path. An example of the calculated areas (white polygons) used to compute the navigation error between the prescribed (magenta) and executed (cyan) paths is presented in Fig. 4. There are two reasons for considering this error as a navigation score rather than an RMS error. First, the executed path is assumed to be a straight line connecting consecutive surfacings, which is not true in general. Hence, we are not actually comparing the true executed path to the precise prescribed path. Second, computing the RMS error requires one to match ( $x, y$ ) coordinates of the executed path with those on the prescribed path in a one-to-one manner. Since the reference path is only composed of 6 waypoints, and the executed paths contain many more waypoints (surfacing locations), this leads to a many-to-one mapping between the paths. If each path is discretized into the same (large) number of points, matching locations between the two paths is still ad-hoc, as the navigational error of the vehicle is quite large.

It is of interest to note that of the experiments considered in Table I, the shortest circuit completion time is associated



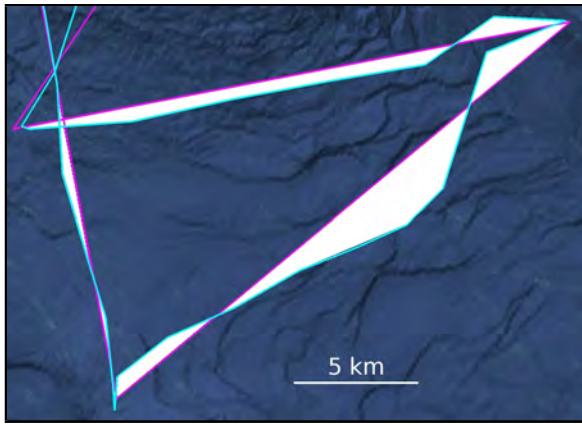


Fig. 4. An example of the calculated areas (white polygons) used to compute the navigation error between the prescribed (magenta) and executed (cyan) paths.

with the longest distance traveled and a navigation score of 0.73 per kilometer. The average speed-over-ground of the glider was 1.16 km/h, which is  $> 0.3$  km/h faster than the average speed observed over multiple years of deployments. This artefact demonstrates the complexity of currents in the ocean and the analysis of repeated execution of a planned path. The execution presented in Fig. 3 traveled an actual distance of 94.5 km, traversed the circuit in 104 hours and 37 min, and had a navigation score of 0.69 km per km traveled.

From Table I, the navigation score for 10 recent executions of the reference path is  $70.35 \text{ km}^2$ , and for each kilometer traveled, the glider is, on average, 0.76 km from the intended location. These results seem poor, however the vehicle is dead-reckoning for up to 8 hours multiple times during the mission. Additionally, these results match well with the results presented in [13], where the authors showed that, in the absence of currents, an expected  $3\sigma$ , crosstrack error over a 2 km transect ( $\sim 160$  minutes underwater) is approximately 0.6 km. With regional currents having an average magnitude  $\sim 20$  cm/s, the data in Table I demonstrate better than expected results. However, we are interested to develop methods that lead to the improvement of these results.

### III. IMPROVED NAVIGATION PLANNING

An obvious method to reduce tracking error is to require the glider to surface more frequently. One could prescribe that the glider surface after each dive to the maximum depth. For our operations, this is not practical. As previously mentioned, we have a minimum time on the surface of 15 minutes. A single single dive (sea surface to 80 m and back to sea surface), given the parameters in Section II-B, takes  $\sim 20$  min. For this extreme scenario, over the course of the deployment a glider would be spending  $> 40\%$  of the time on the ocean surface. Given a 21 day mission, the glider would spend nearly 9 days NOT collecting data. We would prefer the glider to spend less than 10% of the total deployment time on the surface, we desire a reduction in the navigation score in Table I to at most the  $3\sigma = 600$  m crosstrack error presented in [13], and we let  $\delta = 1000$  m. Specifically,

we aim to determine a surfacing interval that reduces, or eliminates the navigation error caused by ocean currents.

Based on recent results in path planning with ocean model predictions ([12], [14], [15]), and to satisfy the above constraints, we consider integrating an unscented Kalman filter with outputs from a regional ocean model. The model outputs provide an environmental uncertainty and allow us to estimate the predicted navigation error for the execution of a given path, thus enabling the computation of appropriate surfacing intervals to ensure bounds on the navigation score and on the total time on the surface. The inputs to the filter are the kinematic glider model, the model output providing 4-dimensional current velocities in the region, and simulated sensor measurements with added zero-mean Gaussian noise.

#### A. Unscented Kalman Filter

Our baseline estimates of the glider dead-reckoning error, in still water, are determined by simulating a typical mission profile, starting at the first waypoint,  $W_1$ , on the desired trajectory. Each dive prescribes  $\phi = 26^\circ$  and  $max = 80$  m. The simulated attitude sensor provides updates at 5 Hz, while the simulated depth sensor provides updates at 1 Hz. We add zero-mean Gaussian noise to each measurement using the RMS sensor accuracy values listed in Section II-A.

We then fuse the measurements from the (simulated) sensors in an unscented Kalman filter (UKF) to estimate the position, attitude and velocity of the vehicle over time [16]. The UKF is a Bayesian filtering algorithm which employs a statistical local linearization procedure to propagate and update the system state. For nonlinear systems, this approach typically produces significantly more accurate estimates than the analytic local linearization employed by the well-known extended Kalman filter (EKF). Our  $10 \times 1$  state vector is

$$\mathbf{x}(t) = \left[ (\mathbf{p}^w(t))^T \quad (\bar{q}_B^w(t))^T \quad (\mathbf{v}^B(t))^T \right]^T \quad (1)$$

where  $\mathbf{p}^w(t)$  is the position of the glider in the world (UTM) frame,  $\bar{q}_B^w(t)$  is the unit quaternion that defines the attitude of the glider body relative to the world frame, and  $\mathbf{v}^B(t)$  is the velocity of the glider in the body frame. This simple kinematic model is sufficient for this application of long-range planning. A primary motivation for our choice of the UKF is its performance with a more sophisticated (and nonlinear) dynamic model of the glider, which we are exploring in a parallel effort.

For our simulation, we assume that the glider follows a nominal linear sawtooth trajectory, and that the vehicle angular rotation rate and linear acceleration are driven by white, zero-mean Gaussian noise processes represented by the vectors  $\eta_q(t)$  and  $\eta_v(t)$ , with covariance matrices  $\mathbf{Q}_q$  and  $\mathbf{Q}_v$  respectively. The system state evolves in continuous time according to

$$\dot{\mathbf{p}}^w(t) = \mathbf{C}(\bar{q}_B^w(t)) \mathbf{v}^B(t) \quad (2)$$

$$\dot{\bar{q}}_B^w(t) = \frac{1}{2} \Omega(\eta_q(t)) \bar{q}_B^w(t) \quad (3)$$

$$\dot{\mathbf{v}}^B(t) = \eta_v(t) \quad (4)$$

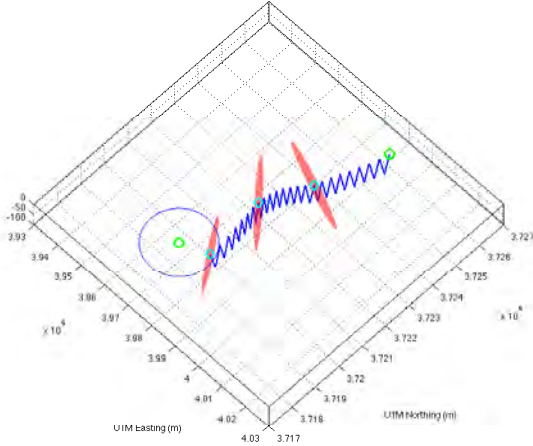


Fig. 5. Estimated trajectory of the glider between waypoints 1 and 2 (along  $\gamma_1$ ), for  $T = 3$  hrs. The trajectory was generated by the UKF; red ellipses indicate the  $3\sigma$  uncertainty bounds for the glider position at each surfacing. The second waypoint is considered to have been *achieved* when the glider surfaces inside the blue circle.

where  $\mathbf{C}(\bar{q}_B^W(t))$  is the direction cosine matrix corresponding to the unit quaternion  $\bar{q}_B^W(t)$ , and  $\Omega(\eta_q(t))$  is the quaternion kinematic matrix, relating the rate of change of the orientation quaternion to the body frame angular velocity [17].

### B. Incorporating Ocean Currents

The ocean model output used in this study is the Regional Ocean Model System (ROMS) run at the Jet Propulsion Laboratory, California Institute of Technology. The model output has three nested horizontal resolutions; the finest (2.2 km) resolution completely covers our area of interest. The vertical resolution is non-uniform, providing data at depths ranging from 0 to 2000 m. For specific details on ROMS, see [18], [19].

The effects of the currents on the glider are incorporated as a concatenation of the contributions from the velocity of the glider in the water column, and the velocity of the water column itself (i.e., the current). The modified process model for the glider position is then

$$\dot{\mathbf{p}}^W(t) = \mathbf{C}(\bar{q}_B^W(t)) \mathbf{v}^B(t) + \mathbf{v}_{\text{ROMS}}(t) \quad (5)$$

where  $\mathbf{v}_{\text{ROMS}}(t)$  is the predicted water current velocity, found by spatiotemporally interpolating the ROMS prediction.

### C. Improved Navigation Strategy

Our improved navigation strategy involves attempting to predict, based on our kinematic model and the ROMS data, how far the glider will drift away from the desired trajectory. We aim to limit the drift such that the distance between the glider's position and the planned trajectory is never larger than the primary axis of the UKF  $3\sigma$  uncertainty ellipse. Equivalently, at least one point on the trajectory should lie within the  $3\sigma$  uncertainty ellipse. For the simulations here,  $3\sigma$  corresponds to  $\sim 600$  m. A 3D representation of the estimated trajectory of the glider between waypoints

1 and 2 (along  $\gamma_1$ ) output by the UKF for  $T = 3$  hours is presented in Fig. 5.

The initial steps follow those for a normal mission. We run a prediction step using a deterministic, discrete kinematic model incorporating ROMS prediction data, for a given surfacing time. The glider begins on the surface, and computes a heading and bearing location  $A_i$  to reach  $W_i$  based on the depth-averaged currents experienced during the previous leg. The glider dives, and surfaces upon reaching  $W_i$  or after a duration  $T$  hours has elapsed.

To begin the simulated mission, we compute an initial depth-averaged current by running for  $T$  hours and finding the offset from the prescribed path as a one-time initialization. This initial drift offset is then used to adjust the glider heading (in the opposite direction) as the difference in angle between our expected and (simulated) trajectory.

Next, we simulate the full dive profile, using ROMS current predictions and the kinematic model above, using the UKF. This provides an expected surfacing location with an associated uncertainty ellipse. If, at the end of  $T$  hours, the glider surfaces more than  $3\sigma$  away from the desired trajectory, the mission terminates. Otherwise, the simulation continues with another dive as outlined in Section II-A.

We iteratively simulate the execution of a segment 25 times;  $T_j = \{2, 2.25, 2.5, \dots, 7.75, 8\}$  hours. For each  $j$ , a path segment with  $T = T_j$ , represent by  $\gamma_i(T_j)$ , is considered successful when the final surfacing on a segment is within  $\delta = 1000$  m of the goal waypoint, and at all surfacings along the segment the distance from the glider to the prescribed path remains less the  $3\sigma$  uncertainty ellipse, i.e., the glider remained within 600 m of the prescribed path. For each  $\gamma_i$ , we compute  $\mathcal{S} = \{\cup_j \gamma_i(T_j) | \gamma_i(T_j) \text{ is successful}\}$ , the set of all successful executions. Then, for the entire path, we compute the desired surfacing interval  $S$  to be

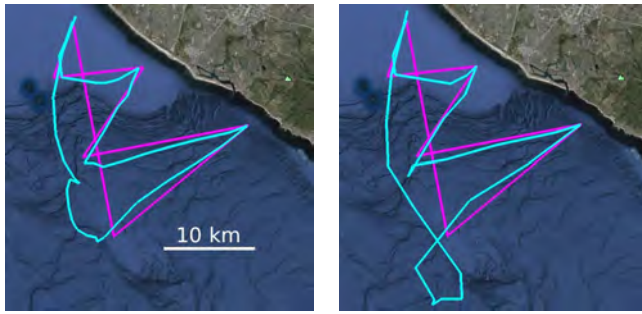
$$S = \min_i \max_j \{T_j | \gamma_i(T_j) \text{ is successful}\} \quad (6)$$

## IV. SIMULATION RESULTS

For the given path  $\gamma$ , we have  $i = 6$  segments joining consecutive waypoints to form our closed-circuit path; magenta path in Fig. 3. In Table II, we present the  $(T_j)$  such that  $\gamma_i(T_j)$  is successful. For all segments, except  $\gamma_6$ , we see that  $2 \leq T \leq 6$  results in a successful completion of the segment. Unfortunately, for the assumed parameters of the simulation,  $\mathcal{S} = \emptyset$  due to  $\gamma_6$  not resulting in a successful execution for any  $T_j$ . Typical of actual conditions, the ROMS output

TABLE II  
TIMES  $T_j$  SUCH THAT  $\gamma_i(T_j)$  IS SUCCESSFUL.

Segment ( $\gamma_i$ )	Acceptable ( $T_j$ )
$\gamma_1$	2, 2.25, $\dots$ , 6.5
$\gamma_2$	2, 2.25, $\dots$ , 6.5
$\gamma_3$	2, 2.25, $\dots$ , 6
$\gamma_4$	2, 2.25, $\dots$ , 6.25
$\gamma_5$	2, 2.25, $\dots$ , 6
$\gamma_6$	$\emptyset$



(a) Simulation results for  $T = 3$  hours. (b) Simulation results for  $T = 6$  hours.

Fig. 6. Two simulation results for the glider following the reference path. The scale shown in Fig. 6(a) is the same for both figures.

predicts strong magnitude currents ( $> 20$  cm/s) throughout the deployment region. In particular, in some areas the ocean currents are stronger than the speed of the glider assumed in the simulation. Thus, there are instances along  $\gamma_6$  when the glider is pushed directly backwards, or computes a very circuitous path to reach the final waypoint. The simulation results corresponding to  $T = 3$  and  $T = 6$  are presented in Fig. 6(a) and 6(b), respectively. For the case when  $T = 3$  hours, the total traversal time is 128.9 hours and the navigation score is 1.19 km. When  $T = 6$  hours, the total traversal time is 145.7 hours and the navigation score is 1.34 km. These predictions do not match well with the previously presented experimental results where  $T = 8$  hours. The traversal times are a bit high, but within  $2\sigma$  of the mean in Table I. The predicted navigation scores are significantly larger than previously experiences in the field. However, if we ignore segment  $\gamma_6$ , then the navigation scores drop to 0.5 and 0.54 for  $T = 3$  and  $T = 6$  hours, respectively. These values compare better with those seen in prior experimental results. A large simulation campaign was conducted over the duration of the field deployment, and similar results were predicted for a range of starting times and surfacing intervals.

In Fig. 7, we present an Empirical Orthogonal Function (EOF) analysis of the deployment region [20]. The analysis was performed on a time-series of 60 consecutive days of ROMS data prior to the deployment time, see [6] for details. Figure 7 represents the temporal variability of the depth-averaged currents in the deployment region. It can be seen that there is significant variability in the currents along  $\gamma_6$ , and at the ends of  $\gamma_3$  and  $\gamma_5$ . Additionally, as can be seen in Fig. 3 that there is a significant change in bathymetry along the gradient of  $\gamma_6$ . This feature is the San Pedro Shelf, and is a well-studied bathymetric feature of the region. Currents are strong, especially upwelling, across this shelf, which makes vehicle navigation difficult. The shelf also makes it very difficult to model the complex current structures occurring due to the extreme changes in the sea floor. It is hypothesized that this is a section of ROMS that is of consistently lower accuracy within the deployment region, as predictions do not match well with field observations.

Assuming that we neglect the prediction for  $\gamma_6$ , we see from Table II that we should choose  $T = 6$  as the constant

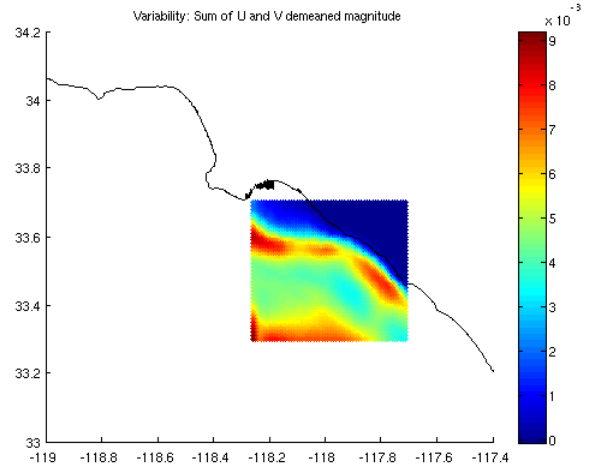


Fig. 7. Empirical Orthogonal Function analysis of 60 days of ROMS data.

TABLE III  
STATISTICS FOR THREE EXECUTIONS OF THE REFERENCE PATH WITH DIFFERENT SURFACING INTERVALS.

Surfacing Interval (hours)	$T = 3$	$T = 4$	$T = 6$
Prescribed Path Length (km)	97.3	68.75	54.54
Actual Distance Traveled (km)	96.94	75.45	61.51
Total Traversal Time (hh:mm)	139 : 19	102 : 47	72 : 54
Navigation Score (km <sup>2</sup> )	36.84	28.78	46.81
Navigation Score per km traveled (km)	0.38	0.38	0.76

surfacing time for execution of the reference path. We are looking for a constant surfacing interval because the glider cannot adapt this parameter on-board and human intervention is required during a glider surfacing to change this parameter; it is very labor-intensive to continually monitor and update the glider missions over a one-month deployment. Also, for safety reasons it is preferable to have the vehicle surface at regularly planned intervals to ensure proper operation.

## V. EXPERIMENTS

The predictions presented in Section IV were tested during sea trials to validate the planning method. Two Slocum gliders were deployed from 19 July 2011 to 1 August 2011. The predictions presented in the previous section were computed, and the reference path (Fig. 1) was simultaneously executed by both vehicles while surfacing at different time intervals. Surfacing intervals of  $T = 3, 4$  and 6 hours were implemented to compare with the predictions presented the Section IV. Figure 8 presents the results of three executions of the reference path. The statistics for the three executed paths is presented in Table III. Due to time constraints and remaining battery life, the simultaneous execution of cases  $T = 4$  and  $T = 6$  had to be terminated before reaching  $\gamma_6$ . This is unfortunate, however we did successfully execute a complete circuit for the case when  $T = 3$ .



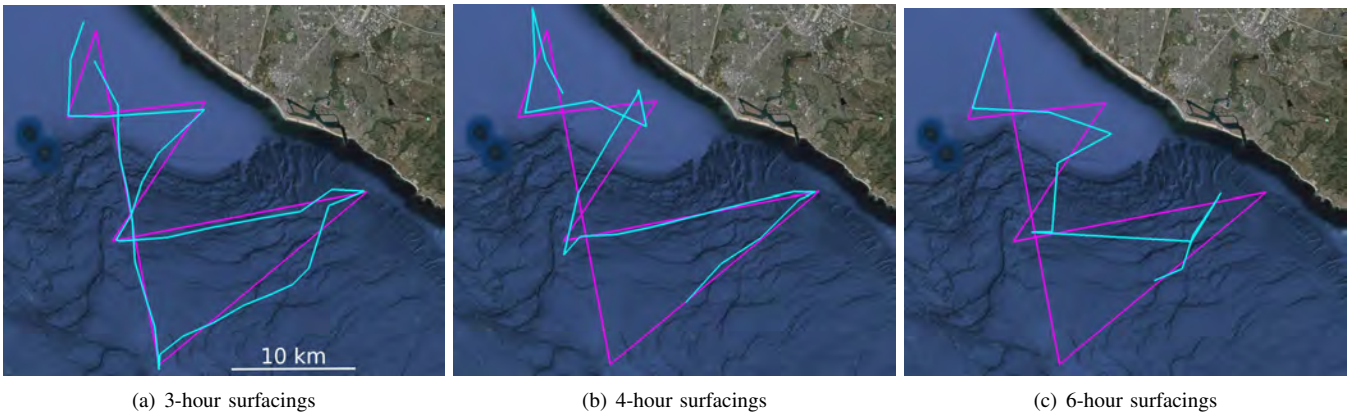


Fig. 8. Executed trajectories for  $T = 3, 4$  and 6-hour surfacing times. The scale in 8(a) is the same for all figures.

As initially predicted, and following intuition, commanding the glider to surface more frequently did result in a decrease in navigation score. It is interesting to note that there is no significant difference in the navigation score between the data presented for  $T = 8$  (Table I) and that for  $T = 6$  hours, however the presented data is not sufficient to provide a comprehensive statistical analysis. For the case of  $T = 3$  hours, we see the navigation score cut in half, and well outside the 3 standard deviations from the mean given in Table I. Additionally, the traversal time of 139 hours is acceptable given the synoptic time-scale of 120 hours. If the gliders were allowed to finish a complete circuit for the cases when  $T = 4$  and  $T = 6$  hours, maintaining the same average velocity, the traversal times would have been  $\sim 123$  hours and  $\sim 109$  hours, respectively. These times are more desirable for the underlying science-driven application of obtaining a synoptic view of the region with respect to algal bloom formation.

From the predictions in Section IV, and the field results given above, we are motivated to choose  $T = 3$  as the surfacing interval for future deployments and executions of the reference path. However, we must be mindful that the vehicle will spend twice as much time on the surface in the case of  $T = 3$  hours than when  $T = 8$  hours. To make an informed decision regarding the safety of the vehicle over the course of a one-month deployment when surfacing every 3 hours, the method presented here could be combined with the risk-aware mission planning presented in [21].

## VI. CONCLUSION

Planning missions and operating an underwater vehicle in a dynamic and complex ocean environment is a challenging task. High levels of uncertainty in the external forces experienced, both in magnitude and direction, along with multiple regional considerations lead to a large set of constraints to consider during the mission design phase. However, all of these factors need to be accounted for to ensure a successful deployment. In this study, we examined the combination of a Kalman filter and regional ocean model output to find a surfacing interval for an autonomous underwater glider, such that the time on the ocean surface and the navigational error have upper bounds. We used a reference path that had

been executed multiple times to provide basic operational guidelines and a benchmark for performance. At this stage of development, there is no guarantee that the proposed technique will find a solution with the posed set of constraints;  $\gamma_6$  is a case in point. However, this failure is directly related to the chosen bound on the desired navigational error, and the structure of the currents in the region. If this constraint is loosened, more times  $T_j$  will exist that make  $\gamma_i$  successful for all  $i$ , since the glider is permitted to deviate more from the prescribed path.

In the simulation presented, we found that  $\gamma_6$  did not have an associated surfacing time such that it could be executed to the desired accuracy. However, when the entire path was executed with the actual robot in the ocean with  $T = 3$  hours, we find that the time on the ocean surface, and overall traversal time are within acceptable limits, while the navigation score improved by 50%. Similar results are observed for  $T = 4$  hours, while the experimental results for  $T = 6$  hours compare with those of multiple trials with  $T = 8$  hours. Although there was only one incomplete trial for  $T = 6$  hours, the data suggest that the surfacing interval should be set to a value less than  $T = 6$  (realistically  $T \approx 3$  hours) to achieve a significant reduction in the navigation score. Although the glider will spend less than 8% of the deployment on the ocean surface for  $T = 3$  hours, this is still more than twice the duration on the surface for  $T = 8$  hours. In the ocean, the chance of collision is small, however we must take care during deployments to ensure the safety of our vehicle as well as the safety of other vehicles and people within the same region.

The results of the simulation compared to the experiments suggests that future developments of the proposed method carry a term that accumulates the navigational error as the simulation progresses, and not only along a single leg. Hence, if the path can be executed very accurately along some segments, we can tolerate slightly higher errors along other segments. It is also of interest to combine this study with the work presented in [6] to determine what magnitude of error is acceptable along each leg, based upon user-input defining the importance of the data gathered along that leg. Specifically, there may be sections of a path that require a

low navigation score and other segments that can be executed with less accuracy.

## VII. FUTURE WORK

The presented work is an initial investigation and experiment into the use of a Kalman filter merged with ocean model predictions to assist in mission planning for autonomous gliders. Further development of this work will be accomplished in three stages. First, we plan to develop an iterative algorithm that will input the glider's last known position, download the updated ROMS prediction each day, compute the surfacing interval time for the next  $\sim 24$  hours, and generate the mission file to be uploaded to the vehicle. Second, we plan to work with ocean scientists with expert domain knowledge to compute appropriate temporally averaged currents, especially in areas near the shelf break region. Based on the complexity of the chosen region, this may result in multiple scenarios due to the annual variability of the currents. Validation of the computations based on the averaged dataset will require extensive field testing over the course of a full year, and is an area the authors are preparing to pursue. Results from all of the field trials will indicate areas for improvement and generate ideas for further extensions of this work. Third, we are interested in examining the sources of discrepancy between the ROMS predictions and the actual currents observed by the vehicle in the ocean. Analysis of the multiple experiments conducted by USC CINAPS that have executed the reference path over the past three years can provide statistically relevant information regarding the accuracy and precision of ROMS predictions in southern California. Such information can be useful for mission planning, as well as for input back to the model for overall improvement.

## VIII. ACKNOWLEDGMENTS

We gratefully acknowledge support from the ONR Antidote MURI project, grant no. N00014-09-1-1031. R.N. Smith and G.S. Sukhatme were also supported in part by the NOAA MERHAB program (grant NA05NOS4781228), NSF as part of the Center for Embedded Network Sensing (CENS) (grant CCR-0120778), and NSF grant CNS-1035866. R.N. Smith was also supported in part by the Early Career Academic Recruitment and Development (ECARD) Program of the Queensland University of Technology. The authors would like to thank Burton H. Jones, Carl Oberg, Bridget Seegers, Matthew Ragan and Arvind Pereira for their valuable assistance with practical science motivations, glider deployment, general operations and data processing. The ROMS predictions used were computed by the Jet Propulsion Laboratory (JPL), California Institute of Technology, under a contract with the National Aeronautics and Space Administration (NASA).

## REFERENCES

[1] H. Singh, A. Can, R. Eustice, S. Lerner, N. McPhee, O. Pizarro, and C. Roman, "Seabed auv offers new platform for high-resolution imaging," *Transactions of the AGU*, vol. 85, pp. 289, 294–295, August 2004.

[2] M. Johnson-Roberson, O. Pizarro, S. B. Williams, and I. Mahon, "Generation and visualization of large-scale three-dimensional reconstructions from underwater robotic surveys," *Journal of Field Robotics*, vol. 27, no. 1, pp. 21–51, 2010.

[3] H. Choset, "Coverage of known spaces: The boustrophedon cellular decomposition," *Autonomous Robots*, vol. 9, pp. 247 – 253, 2000.

[4] A. Singh, A. Krause, C. Guestrin, and W. Kaiser, "Efficient informative sensing using multiple robots," *Journal of Artificial Intelligence Research*, vol. 34, pp. 707–755, 2009.

[5] D. Paley, F. Zhang, and N. Leonard, "Cooperative control for ocean sampling: The glider coordinated control system," *IEEE Transactions on Control Systems Technology*, vol. 16, pp. 735–744, July 2008.

[6] R. N. Smith, M. Schwager, S. L. Smith, B. H. Jones, D. Rus, and G. S. Sukhatme, "Persistent ocean monitoring with underwater gliders: Adapting sampling resolution," *Journal of Field Robotics*, vol. 28, pp. 714 – 741, September/October 2011.

[7] R. N. Smith, J. Das, H. Heidarsson, A. Pereira, I. Cetinić, L. Darjany, M. Ève Garneau, M. D. Howard, C. Oberg, M. Ragan, A. Schnetzer, E. Seubert, E. C. Smith, B. A. Stauffer, G. Toro-Farmer, D. A. Caron, B. H. Jones, and G. S. Sukhatme, "USC CINAPS builds bridges: Observing and monitoring the Southern California Bight," *IEEE Robotics and Automation Magazine, Special Issue on Marine Robotics Systems*, vol. 17, pp. 20–30, March 2010.

[8] Webb Research Corporation. <http://www.webbresearch.com/slocum.htm>, 2008. viewed March 2011.

[9] O. Schofield, J. Kohut, D. Aragon, E. Creed, J. Graver, C. Haldman, J. Kerfoot, H. Roarty, C. Jones, D. Webb, and S. Glenn, "Slocum gliders: Robust and ready," *Journal of Field Robotics*, vol. 24, no. 6, pp. 473–485, 2007.

[10] G. Griffiths, C. Jones, J. Ferguson, and N. Bose, "Undersea gliders," *Journal of Ocean Technology*, vol. 2, no. 2, pp. 64–75, 2007.

[11] R. E. Davis, M. Ohman, D. Rudnick, J. Sherman, and B. Hodges, "Glider surveillance of physics and biology in the southern California current system," *Limnol. Oceanogr.*, vol. 53, no. 2, pp. 2151–2168, 2008.

[12] R. N. Smith, Y. Chao, P. P. Li, D. A. Caron, B. H. Jones, and G. S. Sukhatme, "Planning and implementing trajectories for autonomous underwater vehicles to track evolving ocean processes based on predictions from a regional ocean model," *International Journal of Robotics Research*, vol. 29, pp. 1475–1497, October 2010.

[13] R. N. Smith, J. Kelly, Y. Chao, B. H. Jones, and G. S. Sukhatme, "Towards improvement of autonomous glider navigation accuracy through the use of regional ocean models," in *Proceedings of the 29th International Conference on Offshore Mechanics and Arctic Engineering*, (Shanghai, China), pp. 597–606, June 2010.

[14] J. Witt and M. Dunbabin, "Go with the flow: Optimal path planning in coastal environments," in *Proceedings of the 2008 Australasian Conference on Robotics & Automation (ACRA 2008)* (J. Kim and R. Mahony, eds.), (Canberra, ACT), 2008. ISBN: 9780646506432.

[15] D. R. Thompson, S. Chien, A. Balasurayya, S. Petillo, Y. Chao, P. Li, B. Cahill, J. Levin, M. Meisinger, M. Arrott, and O. Schofield, "Spatiotemporal path planning in strong, dynamic, uncertain currents," in *Proceedings of the IEEE International Conference on Robotics and Automation*, pp. 4778 – 4783, 2010.

[16] S. J. Julier and J. K. Uhlmann, "Unscented filtering and nonlinear estimation," *Proceedings of the IEEE*, vol. 92, pp. 401–422, March 2004.

[17] B. L. Stevens and F. L. Lewis, *Aircraft Control and Simulation*. Wiley-Interscience, Second ed., October 2003.

[18] A. F. Shchepetkin and J. C. McWilliams, "The regional oceanic modeling system (ROMS): a split-explicit, free-surface, topography-following-coordinate oceanic model," *Ocean Modelling*, vol. 9, pp. 347–404, 2005.

[19] Y. Chao, Z. Li, J. Farrara, J. C. McWilliams, J. Bellingham, X. Capet, F. Chavez, J.-K. Choi, R. Davis, J. Doyle, D. Frantaoni, P. Li, P. Marchesiello, M. Moline, J. Paduan, and S. Ramp, "Development, implementation and evaluation of a data-assimilative ocean forecasting system off the central California coast," *Deep-Sea Research II*, vol. 56, 2008.

[20] I. Holmstrom, "Analysis of time series by means of empirical orthogonal functions," *Tellus*, vol. XXII, pp. 638 – 647, 1970.

[21] A. A. Pereira, J. Binney, B. H. Jones, M. Ragan, and G. S. Sukhatme, "Toward risk aware mission planning for autonomous underwater vehicles," in *IEEE/RSJ International Conference on Intelligent Robots and Systems*, Sep 2011.